

Effect of Adsorption by Cellulose Acetate Membrane on Reverse Osmosis of Some Monoamino Monocarboxylic and Monoamino Dicarboxylic Acids in Aqueous Solutions

Osami TOZAWA* and Danji NOMURA

Department of Food Science and Technology, Faculty of Agriculture, Kyushu University,
Hakozaki, Higashi-ku, Fukuoka 812

(Received March 4, 1982)

Taft's polar and steric parameters, $\Sigma\sigma^*$, ΣE_s , and nonpolar parameter, ΣS^* governing the reverse osmosis of nonionized polar aliphatic and alicyclic organic compounds using a cellulose acetate membrane were also applicable to aliphatic monoamino monocarboxylic acids having zwitter ion structure. These three parameters were further extended so as to include the cases of sulfur-containing amino acids, hydroxy-substituted, and aromatic type amino acids. Reverse osmosis of monoamino monocarboxylic acids in binary aqueous solution systems containing L-alanine was carried out. As a result, added amino acids were adsorbed by the membrane when added in low concentration (<0.001 mol dm⁻³), and the permeation of L-alanine was governed by the difference of Taft's polar parameter between L-alanine and the added amino acid. Reverse osmosis of monoamino dicarboxylic acids indicated that hydrogen ions were adsorbed by the membrane, and the adsorption isotherms of hydrogen ions were approximately represented by the Langmuir formula for each amino acid. The electrostatic repulsion between R⁻ ionic species in monoamino dicarboxylic acid and the negatively dissociated groups of the membrane was weakened by neutralization of the membrane by hydrogen ion adsorption, resulting in decreased amino acid rejection. It was noted that the ultraviolet spectrum and the titration curve of permeate of amino acids were different from those of the feed solution; relationship between this phenomenon and adsorption of hydrogen ions was investigated.

Reverse osmosis and ultrafiltration methods have been used for the concentration of protein solutions, purification of enzymes, *etc.* When enzymatic processes are conducted in an ultrafiltration reactor however, pretreatment of the membrane with deposition of inert proteinic gel onto the membrane surface is necessary because the enzyme is inactivated when adsorbed on the surface of a membrane.¹⁻³⁾ It is further reported that the adsorption of solutes at a membrane-solution interface results in the formation of a gel layer; this causes difficulty in washing the membrane.⁴⁾ These studies indicate that adsorption of solutes by a membrane is one of the major problems in reverse osmosis and ultrafiltration processes.

It has been reported that a variety of substances can be adsorbed on cellulosic materials, *i.e.*, adsorption of *m*-aminobenzoic acid on cellulose acetate powder,⁵⁾ cellulose-triacetate and cellulose-acetate-butyrate on porous adsorbents (calcium silicate or aluminum silicate),⁶⁾ sulfobromophthalein sodium on regenerated cellulose membrane which immobilizes activated charcoal.⁷⁾ Literature further reports that surface flow of *p*-chlorophenol⁸⁾ and cumene⁹⁾ is caused by their adsorption on a cellulose acetate membrane. Little work has been done so far to explain the mechanism of ionic permeation through a membrane on which adsorption layer is formed.

The purpose of this study is to explain, on the basis of preferential sorption-capillary flow mechanism,¹⁰⁾ the effect of adsorption of ions at the membrane-solution interface during permeation of amino acids through a cellulose acetate membrane.

In the previous papers,¹¹⁻¹⁴⁾ a number of the following facts were elucidated: (a) Factors governing the reverse osmosis of monoamino monocarboxylic acids in a single system; (b) effect of adsorption of an added amino acid on reverse osmosis of monoamino monocarboxylic acids in binary aq. solutions systems con-

taining L-alanine and (c) the effect of adsorption of hydrogen ions on reverse osmosis of monoamino dicarboxylic acids in single system.

In this paper, the effects of adsorption of hydrogen ions is explained by measuring the UV spectrum and the titration curve of the permeate, are summarized along with previous work.

Transport Equations

Rejection, η is defined as follows:

$$\eta \equiv \frac{C_2 - C_3}{C_2} \quad (1)$$

where C_2 and C_3 refer to the concentration at the membrane-solution interface and in the permeate, respectively. Generally, C_2 differs from the concentration in the feed solution, C_1 . C_2 can be expressed as¹⁵⁾

$$C_2 = C_3 + (C_1 - C_3) \exp\left(-\frac{N_w + N_s}{c_1 k}\right) \quad (2)$$

where c_1 is the molar density of the feed solution, k is the mass transfer coefficient, and N_w and N_s refer to the molar flux of water and solute, respectively. k depends on the shape of the reverse osmosis cell and the streaming state of solution in the cell. On the cell used in this study, k can be represented as follows:¹¹⁾

$$k = 7.586 \left(\frac{D}{l}\right) R_e^{0.420} S_c^{1/3} \quad (3)$$

where D is the diffusivity, l is the inside diameter of the cell, R_e is the Reynolds number, and S_c is the Schmidt number. The solute transport parameter, $D/K\delta$ is defined as¹⁵⁾

$$D/K\delta \equiv \frac{N_s}{C_2 - C_3} = \frac{JC_3}{C_2 - C_3} = J \left(\frac{1}{\eta} - 1 \right) \quad (4)$$

where J is the volume flux of permeate.

Experimental

Amino Acids and Membranes. Reagent grade amino acids were used. DDS-600, 800, 870, and 880 cellulose acetate membranes (Loeb type, De Danske Sukkerfabrikker, Denmark) were used. Cellulose acetate (Eastman 398-3) membranes were also prepared according to the method developed by Manjikian.¹⁶⁾

Analysis and Procedures. The concentration of amino acid in single aq solution was measured with ninhydrin method using a Hitachi spectrophotometer, model 100-30. Amino acids in binary aq solution were analyzed by paper or thin-layer chromatography, using a DMU-33C densitometer (Toyo Kagaku Sangyo, Inc.). The concn of sodium chloride was measured with a MS conductivity bridge CD-35MII. Hydrogen ion concn was determined by using a Hitachi-Horiba F-7Lc pH meter. UV spectra were recorded with a UV-300 spectrophotometer (Shimadzu Seisakusho, Inc.). The titration curve was determined with a UCB-7 automatic titrator (Hiranuma Sangyo, Inc.). Experiments were conducted in a batch using a stirred reverse osmosis cell (Bio Engineering RO-3). The volume and effective membrane area were 200 cm³ and 32.2 cm², respectively. The stirrer was rotated at 300 min⁻¹ by magnetic force. When constant permeation of the membrane was achieved, a 2500 cm³ volume reservoir was attached to the cell. The cell was immersed in a water bath kept at 30 °C. The operating pressure was 1.96 MPa. Figure 1 shows the relationship between η of 0.085 mol dm⁻³ of sodium chloride aq solution and the pure water permeability, A obtained by using a cellulose acetate membrane. Figure 1 shows that the property of a DDS-membrane is the same as that of a laboratory-made membrane. Before the experiments, membranes were always tested with distilled water and 0.085 mol dm⁻³ of sodium chloride aq solution, and the relationship shown in Fig. 1 was confirmed.

Results and Discussion

Factors Governing Permeation of Monoamino Monocarboxylic Acids in a Single System. A monoamino monocarboxylic acid existing as zwitter ion in aq solution possesses zero net charge. Therefore, Eq. 5 proposed by Matsuura *et al.*¹⁷⁾ for the solute transport parameter, $D/K\delta$ of nonionized polar aliphatic and alicyclic compounds is employed to determine the factors governing

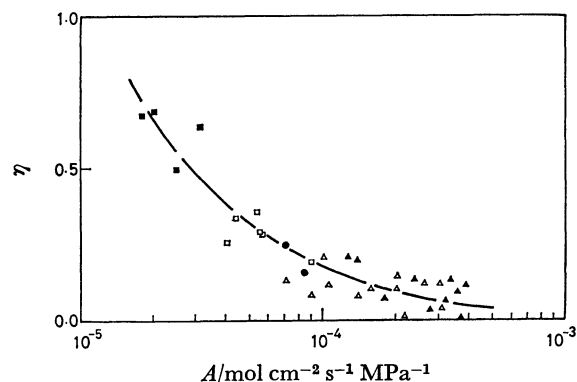


Fig. 1. Relation between η and A for 0.085 mol dm⁻³ of NaCl aq soln.
 △: DDS-600, ▲: DDS-800, □: DDS-870, ■: DDS-880, ●: laboratory-made.

the reverse osmosis of monoamino monocarboxylic acids (0.001 mol dm⁻³):^{11,12)}

$$\ln (D/K\delta) = \ln C^* + \rho^* \Sigma \sigma^* + \delta^* \Sigma E_s + \omega^* \Sigma S^*. \quad (5)$$

D is the diffusivity, δ is the effective thickness of the membrane, K is the reciprocal of the distribution coefficient, and $\ln C^*$ is constant, depending on the porous structure of the membrane surface, the chemical nature of the membrane material, and the nature of the functional group in the solute molecule; $\rho^* \Sigma \sigma^*$, $\delta^* \Sigma E_s$, and $\omega^* \Sigma S^*$ refer to polar, steric, and non-polar effects, respectively; $\Sigma \sigma^*$, Taft's polar parameter; ΣE_s , Taft's steric parameter; ΣS^* , nonpolar parameter (modified Small's number); and ρ^* , δ^* , and ω^* are the characteristic proportionality constants associated with $\Sigma \sigma^*$, ΣE_s , and ΣS^* , respectively. ρ^* and ω^* do not depend on the porous structure of the membrane surface, whereas δ^* depends on the porosity of the membrane. $\Sigma \sigma^*$ and ΣE_s for a variety of substituents are tabulated in Taft's table,¹⁸⁾ however, the number of substituents listed is not enough, on the other hand, ΣS^* is applicable to substituents composed of hydrocarbons only.⁹⁾ Therefore, in order to apply Eq. 5 to sulfur-containing, hydroxy-substituted, and aromatic type amino acids, it is necessary to correlate the characteristic parameters ($\Sigma \sigma^*$, ΣE_s , and ΣS^*) with other physical quantities. The proportion of the ionic bond in an optional substituent can be calculated by measuring the polarity between diverse atoms.¹⁹⁾ $\Sigma \sigma^*$ was a correlation on the basis of the ionic bond proportion. Steric effects depend on the size and shape of the solute molecule. Hence, ΣE_s was correlated on the basis of the molecular weight of the substituent. On the other hand, a nonpolar effect would depend on a hydrophobic interaction energy between the membrane and solute, called an interaction energy of London-van der Waals dispersion force. ΣS^* was a relationship of interaction energy. The values of the parameters obtained are tabulated in Table 1. The nonpolar effect is considered negligible if the molecular structure of the solute contains a straight chain involving no more than three carbon atoms not associated with a polar functional group.¹⁷⁾ For glycine and L-alanine, Eq. 5 can be reduced to

$$\ln (D/K\delta) = \ln C^* + \rho^* \Sigma \sigma^* + \delta^* \Sigma E_s. \quad (6)$$

As $\Sigma \sigma^*$ and ΣE_s in L-alanine are zero, $\ln C^*$ can be expressed as

$$\ln C^* = \ln (D/K\delta)_{\text{L-alanine}}. \quad (7)$$

From Eqs. 6 and 7, we have

$$\delta^* = \frac{\ln (D/K\delta)_{\text{glycine}} - \ln (D/K\delta)_{\text{L-alanine}} - \rho^* (\Sigma \sigma^*)_{\text{glycine}}}{(\Sigma E_s)_{\text{glycine}}}, \quad (8)$$

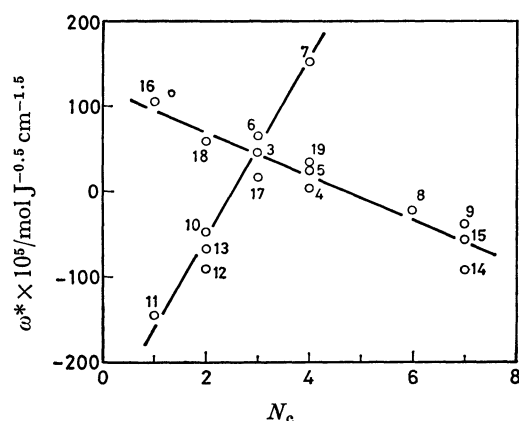
where the reaction constant in the hydrolysis reaction of the ester (=1.465)¹⁸⁾ was employed as a numerical value of ρ^* . From Eq. 5, ω^* can be expressed as follows:

$$\omega^* = \frac{\ln (D/K\delta) - \ln C^* - \rho^* \Sigma \sigma^* - \delta^* \Sigma E_s}{\Sigma S^*}. \quad (9)$$

ω^* is correlated with the number of carbon atoms in

TABLE 1. SUMMARY OF PHYSICOCHEMICAL PROPERTIES OF SOME AMINO ACIDS

Number	Amino acid	ΣE_s	$\Sigma \sigma^*$	ΣS^*	$k \times 10^4$
				$\text{J}^{0.5} \text{cm}^{1.5} \text{mol}^{-1}$	cm s^{-1}
1	Glycine	1.24	0.490	184	78
2	L-Alanine	0.00	0.000	438	70
3	L-Valine	-0.47	-0.190	933	61
4	L-Leucine	-0.93	-0.125	1205	57
5	L-Isoleucine	-1.13	-0.210	1205	57
6	DL-Norvaline	-0.36	-0.115	982	61
7	DL-Norleucine	-0.39	-0.130	1254	57
8	D-Phenylglycine	-2.55	0.600	685	57
9	L-Phenylalanine	-0.38	0.215	957	55
10	DL-2-Aminobutyric acid	-0.07	-0.100	710	65
11	L-Serine	-0.18	0.555	415	67
12	L-Threonine	-0.30	0.530	696	62
13	L-Homoserine	-0.30	0.530	696	62
14	L-Tyrosine	-0.38	0.800	980	53
15	Dopa	-0.46	0.600	1066	52
16	L-Cysteine	-0.32	-0.400	661	64
17	L-Methionine	-0.46	-0.290	1236	57
18	DL-Homocysteine	-0.40	-0.360	939	59
19	DL-Ethionine	-0.50	-0.250	1530	54

Fig. 2. Relation between ω^* and N_e .

Number is solute number of amino acid, membrane: DDS ($A = 8.16 \times 10^{-5} \text{ mol cm}^{-2} \text{ s}^{-1} \text{ MPa}^{-1}$).

a substituent, N_e , as shown in Fig. 2. ω^* of aliphatic amino acids having straight chain and hydroxy-substituted amino acids varies as the number of carbon atoms, but ω^* of aliphatic amino acids having branched chain, sulfur-containing amino acids and aromatic amino acids varies inversely with the number of carbon atoms. These relations are approximated by a first-order equation as follows:

for the former,

$$\omega^* = -2.66 \times 10^{-3} + (1.05 \times 10^{-3})(N_e), \quad (10)$$

for the latter,

$$\omega^* = 1.19 \times 10^{-3} - (2.54 \times 10^{-4})(N_e). \quad (11)$$

By using Eqs. 4, 5, 7, 8, 10, and 11, rejection values of each amino acid are calculated, and compared with the real values, as is shown in Fig. 3. The calculated values are in fair agreement with the real values, which shows that polar, steric, and nonpolar effects all play

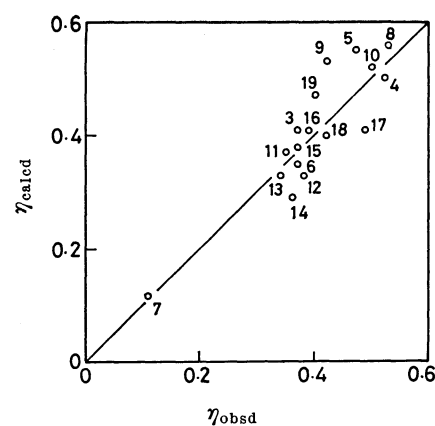


Fig. 3. Calculation of rejection of amino acid.

Number is solute number of amino acid, membrane: DDS ($A = 8.16 \times 10^{-5} \text{ mol cm}^{-2} \text{ s}^{-1} \text{ MPa}^{-1}$).

some role in the reverse osmosis of monoamino monocarboxylic acids. It is further noted that the order of rejection of amino acids is nearly consistent with Matsuura and Sourirajan's data²⁰ (Laboratory-made Batch 316 (10/30)-type cellulose acetate membrane).

Interaction between Two Monoamino Monocarboxylic Acids on a Membrane-solution Interface.

The reverse osmosis of fourteen kinds of solution consisting of L-alanine ($0.001 \text{ mol dm}^{-3}$) and added amino acids (0.00025 — $0.004 \text{ mol dm}^{-3}$) of aliphatic, hydroxy-substituted, sulfur-containing, and aromatic types has been reported in a previous paper.¹³ The results show that the rejection of L-alanine is almost constant in the concentration range (0.001 — $0.004 \text{ mol dm}^{-3}$) in all the systems, except when the concentration of the acids is decreased to $0.00025 \text{ mol dm}^{-3}$, the rejection of L-alanine increases considerably. Rejection of the added amino acids is almost constant through out the con-

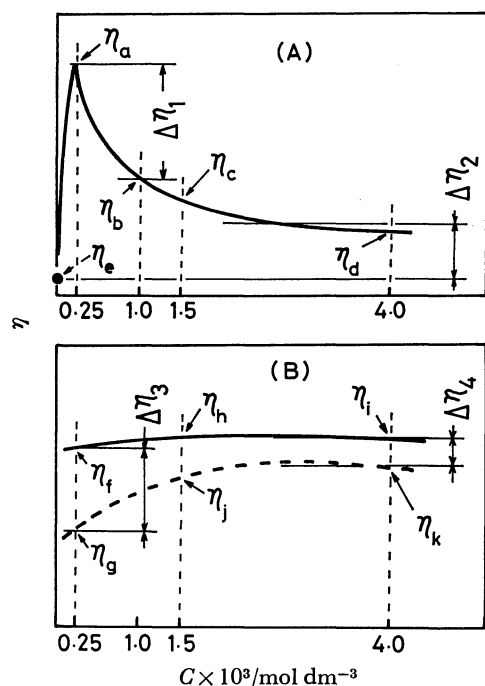


Fig. 4. Schematic diagram of reverse osmosis.
(A): L-Alanine, (B): added amino acid, solid line:
binary system, broken line: single system.

concentration range of 0.00025–0.004 mol dm⁻³ in most of the systems. On the other hand, in a single system, rejection of amino acids is almost constant in the concentration range of 0.001 to 0.004 mol dm⁻³, but decreases when the concentration of the amino acid decreases below 0.001 mol dm⁻³. Figure 4 shows the schematic diagram of the reverse osmosis systems mentioned above. The four equations shown below represent the change in the rejection pattern of these amino acids:

$$\Delta\eta_1 \equiv \eta_a - \eta_b, \quad (12)$$

$$\Delta\eta_2 \equiv (\eta_c + \eta_d)/2 - \eta_e, \quad (13)$$

$$\Delta\eta_3 \equiv \eta_f - \eta_g, \quad (14)$$

$$\Delta\eta_4 \equiv (\eta_h + \eta_i)/2 - (\eta_j + \eta_k)/2, \quad (15)$$

where $\eta_a, \eta_b, \dots, \eta_j$, and η_k are shown in Fig. 4. $\Delta\eta_1, \Delta\eta_2, \Delta\eta_3$, and $\Delta\eta_4$ are used in order to summarize experimental data of rejection in many systems. $\Delta\eta_1, \Delta\eta_2, \Delta\eta_3$, and $\Delta\eta_4$ in each system are tabulated in Table 2. A glance at Table 2 shows that $\Delta\eta_1, \Delta\eta_2, \Delta\eta_3$, and $\Delta\eta_4$ are positive in most of the systems. Therefore, the rejection of both L-alanine and the added amino acids is higher in a binary system than in a single system. On the other hand, $\Delta\eta_1$ is greater in systems consisting of L-alanine and aliphatic amino acid than in the other systems. $\Delta\eta_1$ is correlated by $\Sigma\sigma^*$ of each added amino acid, as shown in Fig. 5. When $\Sigma\sigma^*$ of the added amino acid and that of L-alanine are close to each other, rejection of L-alanine increases considerably, but when they are further apart, rejection of L-alanine is not much effected. In the single systems shown in Fig. 6, rejection of some amino acids, (especially aliphatic amino acids) shifts from positive to negative as the concn. of feed solution decreases from 0.001 to 0.00025 mol dm⁻³. It has been reported

TABLE 2. DIFFERENCE BETWEEN AMINO ACID REJECTION IN BINARY AND SINGLE SYSTEMS^{a)}

Added amino acid	$\Delta\eta_1$	$\Delta\eta_2$	$\Delta\eta_3$	$\Delta\eta_4$
L-Serine	0.02	0.10	0.15	0.15
L-Threonine	0.08	0.11	0.09	-0.09
DL-2-Aminobutyric acid	0.21	0.11	0.89	0.05
DL-Norleucine	0.52	0.23	0.46	0.00
DL-Norvaline	0.26	0.03	-0.17	0.15
L-Leucine	0.30	0.23	0.44	0.03
L-Valine	0.34	0.11	0.90	0.21
L-Isoleucine	0.16	0.06	0.08	-0.11
L-Methionine	0.03	0.21	0.35	0.02
DL-Ethionine	0.06	0.27	0.48	0.28
DL-Homocysteine	0.04	0.35	—	—
L-Phenylalanine	0.09	0.09	0.12	0.14
D-Phenylglycine	0.02	0.10	0.14	-0.12
L-Tyrosine	0.14	0.00	0.13	0.24

a) The membrane is DDS membrane ($A = 8.16 \times 10^{-5}$ mol cm⁻² s⁻¹ MPa⁻¹).

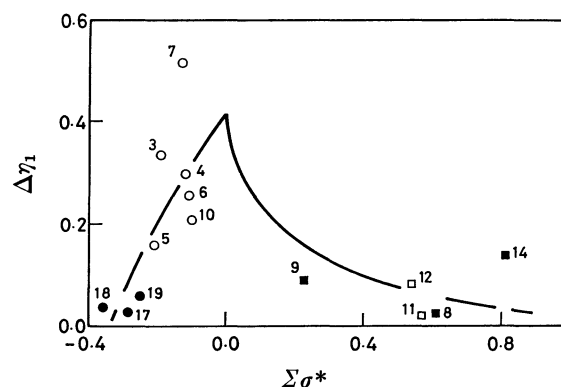


Fig. 5. Effect of Taft's polar parameter on $\Delta\eta_1$.
Number is solute number of amino acid, ○: aliphatic type, ●: sulfur-containing type, □: hydroxy-substituted type, ■: aromatic type, membrane: DDS ($A = 8.16 \times 10^{-5}$ mol cm⁻² s⁻¹ MPa⁻¹).

in the literature that the molar surface tension increment of aliphatic amino acids decreases as the length of the hydrocarbon side chain increases. For example, the molar increment of surface tension is positive for glycine and alanine, but negative for 2-aminobutyric acid, valine, and 2-aminohexanoic acid, showing that 2-aminobutyric acid, valine, and 2-aminohexanoic acid are positively adsorbed at the liquid surface in accordance with Gibbs' theorem.^{21,22)} These facts reflect that the typical behavior of amino acids is attributed to the surface flow of amino acids caused by the formation of an adsorption layer of amino acids on a surface of the membrane near 0.00025 mol dm⁻³. On the basis of the assumption mentioned above, the relation between $\Delta\eta_1$ and $\Sigma\sigma^*$ of added amino acids shown in Fig. 5 is explained below. In the first place, for systems consisting of L-alanine and aliphatic amino acids, L-alanine interacts with the adsorption layer of the aliphatic amino acid. But, L-alanine does not have

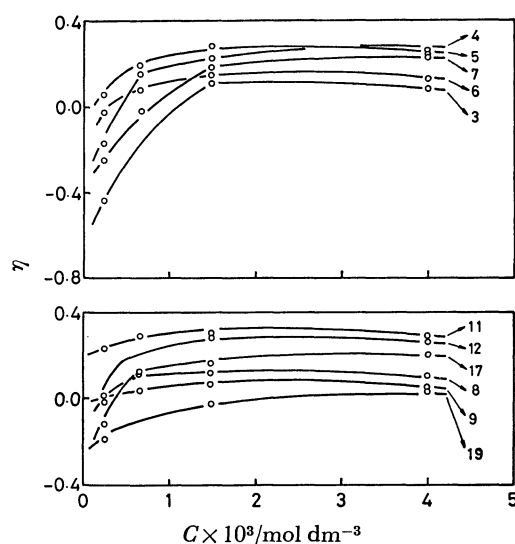


Fig. 6. Effect of concentration on rejection for single system.

Number is solute number of amino acid, membrane : DDS-600.

a strong affinity for the adsorption layer because the Taft's polar parameter of the aliphatic amino acid and that of L-alanine are close to each other, *i.e.*, the acidity of the aliphatic amino acid is approximately equal to that of L-alanine. Therefore, rejection of L-alanine increases at the concn of the added amino acids ($0.00025 \text{ mol dm}^{-3}$). In the case of systems consisting of L-alanine and added amino acids of hydroxy-substituted, sulfur-containing, and aromatic types, the adsorption layer is formed, but, L-alanine has a strong affinity for the adsorption layer according to Taft's polar parameter, hence, rejection of L-alanine is unaffected.

Hydrogen Ion Adsorption during Permeation of Monoamino Dicarboxylic Acids. The results of the reverse osmosis of monoamino dicarboxylic acids in aq solution have been reported in a previous paper in order to study the adsorption of hydrogen ions on the membrane.¹⁴⁾ Figure 7 shows the result of reverse osmosis of L-glutamic acid. The high pH of the L-glutamic acid permeate solution (16 cm^3 of initial permeate) as compared to that of feed solution is prominent in the low concentration range. This can be explained on the basis that a cellulose acetate membrane is slightly negatively charged,²³⁾ therefore, hydrogen ions become adsorbed on its surface. In the case of the initial permeate, rejection increases as the concentration of the feed solution decreases. This behavior is considered to be due to the higher electrostatic repulsion force between the membrane and the R^- ion of L-glutamic acid. An electrostatic repulsion force is also reported in case of lower organic acids,²⁴⁾ however, these authors considered the cellulose acetate membrane to be a non charged membrane, and they used a dielectric exclusion force to explain the above phenomenon. To confirm this fact that a cellulose acetate membrane has a weak ion-exchange character, an experiment on the adsorption of Methylene Blue and erioglaucine A on the membrane was carried out. As a result, positively charged oxidation type ions were more abun-

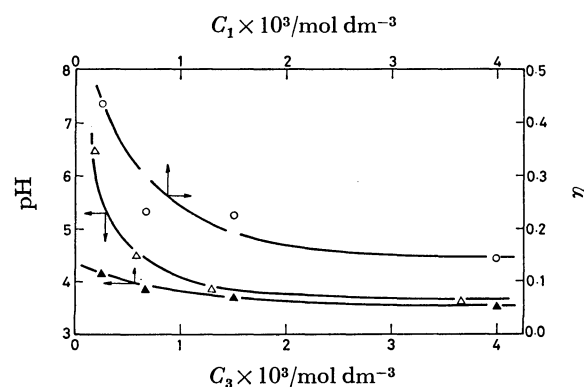


Fig. 7. pH change in reverse osmosis of L-glutamic acid in aq soln.

○: Rejection of L-glutamic acid, ▲: pH of feed soln, △: pH of permeate (16 cm^3 of initial product), membrane : DDS-600.

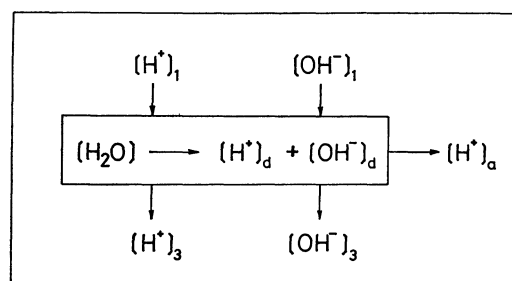


Fig. 8. Adsorption model of hydrogen ion.

Subscript 1: feed soln, 3: permeate, a: adsorption, d: dissociation, □: membrane.

dantly adsorbed than non charged reduction type ions. The adsorption model is shown in Fig. 8 in order to describe quantitatively the adsorption of hydrogen ions under the reverse osmosis. Hydrogen ions produced from a monoamino dicarboxylic acid and hydroxide ions enter the membrane, whereas, only hydrogen ions are adsorbed, resulting in the dissociation of a part of the water within the membrane. We assume the dissociation of water to explain this phenomenon because the ionic product of water represented by Eq. 16 has to be applied to the permeate:

$$K_w = [H^+][OH^-]. \quad (16)$$

Applying a material balance of hydrogen and hydroxide ions to a unit volume of solution which permeate through the membrane, we obtain

$$[H^+]_3 = [H^+]_1 - [H^+]_a + [H^+]_d, \quad (17)$$

$$[OH^-]_3 = [OH^-]_1 + [OH^-]_d, \quad (18)$$

where subscripts 1, 3, a, and d refer to the feed solution, permeate, adsorption, and dissociation, respectively. $[H^+]_1$ is essentially the hydrogen ion concentration in the amino acid solution not permeated through the membrane whose amino acid concentration is the same as that of the permeate. However, in this study we consider it as the hydrogen ion concentration in the feed solution because the rejection is low; in other words, C_1 is approximately equal to C_3 . Assuming that the hydrogen ion and hydroxide ion concentrations in the pores of membrane are iden-

tical with those in the permeate, the electrical neutrality condition can be expressed as follows:

$$[H^+]_3 + [R^+] = [R^-] + 2[R^{2-}] + [OH^-]_3 + [X^-], \quad (19)$$

where $[R^+]$, $[R^-]$, and $[R^{2-}]$ are the concentrations of each ionic species in the monoamino dicarboxylic acid, and $[X^-]$ is the concentration of the negatively dissociated group not adsorbed by hydrogen ions. Inserting Eqs. 17 and 18 in Eq. 19, we have

$$[H^+]_1 - [H^+]_a + [H^+]_d + [R^+] = [R^-] + 2[R^{2-}] + [OH^-]_1 + [OH^-]_d + [X^-]. \quad (20)$$

Here, we have

$$[H^+]_d = [OH^-]_d. \quad (21)$$

From Eqs. 20 and 21, the electrical neutrality condition in the pores can be represented also as follows:

$$[H^+]_a = [H^+]_1 - [OH^-]_1 + [R^+] - [R^-] - 2[R^{2-}] - [X^-]. \quad (22)$$

Using Eqs. 16, 17, 18, and 21, amount of adsorbed hydrogen ion, M can be derived as follows:

$$M = \int_0^V [H^+]_a dV = \int_0^V \left[K_w \left(\frac{1}{[H^+]_3} - \frac{1}{[H^+]_1} \right) + [H^+]_1 - [H^+]_3 \right] dV, \quad (23)$$

where V is permeate volume. When the permeation proceeds to the permeate volume where $[H^+]_a$ is zero, i.e., $[H^+]_1$ is equal to $[H^+]_3$, the adsorption of hydrogen ions stop. Then $[H^+]_1$ is in equilibrium with an equilibrium amount of adsorbed hydrogen ions, M_e . Figure 9 shows the adsorption isotherm of hydrogen ions of each amino acid. The adsorption isotherm may be represented by the Langmuir formula given by

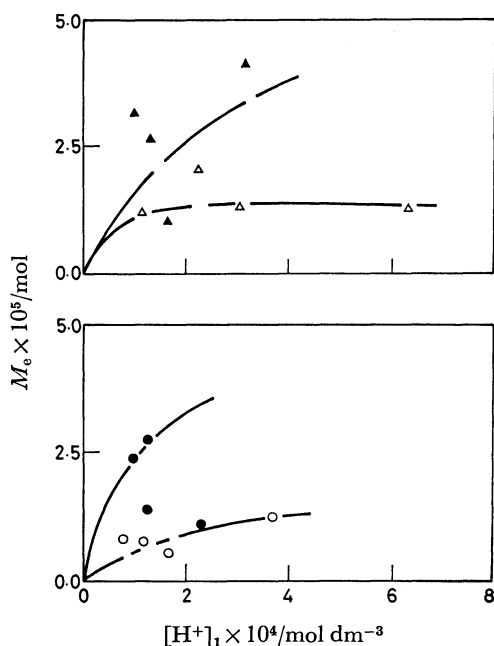


Fig. 9. Adsorption isotherm of the hydrogen ion.
○: L-Glutamic acid, △: L-aspartic acid, ▲: DL-2-aminoadipic acid, ●: DL-2-aminopimelic acid, membrane: DDS-600.

$$M_e = \frac{ab[H^+]_1}{1 + a[H^+]_1}, \quad (24)$$

where a and b are constants. Figure 9 shows some variation because the data were taken from the permeate solution, whereas, in the case of the sorption method, the adsorption of hydrogen ions could hardly be noted. The amount required to saturate the unit volume of the membrane is about 0.03 mol dm^{-3} for L-glutamic acid and L-aspartic acid. This value is in fair agreement with the fixed-charge concentration, $0.010 \text{ mol dm}^{-3}$ reported by Igawa *et al.*²⁵⁾ The effect of the adsorption of hydrogen ions in the case of monoamino dicarboxylic acids permeation is shown in Fig. 10. In the case when the membrane approaches equilibrium quickly, an electrostatic repulsion force between the ionic species R^- and the dissociated groups of the membrane is weakened by the neutralization of the membrane with hydrogen ions, resulting in a decrease of the rejection and approaches a constant value as permeation proceeds. On the other hand, when the amount of adsorbed approaches equilibrium slowly, rejection is almost constant because the charge density of the membrane is not changed so much with adsorption of hydrogen ions.

Ultraviolet Spectrum and Titration Curve of Permeate of Amino Acids. UV spectra of the permeate of each monoamino dicarboxylic acid are shown in Fig. 11.

The initial permeates exhibit their absorption maxima at a wavelength of 255 nm, however, the absorption maxima disappear as the permeation proceeds. When the concentration of the feed solution is high, the above maxima are smaller. The permeate volume of each amino acid where the absorption maxima vanish, is roughly the same as that in which $[H^+]_a$ is zero, as mentioned earlier. As a general rule, the absorption of the carboxyl group is obscured by the amino auxochrome whose absorption is very strong, therefore, the absorption maxima do not appear in α type of amino acids. But as mentioned above, the absorption maxima appear in amino acid solutions permeated through the

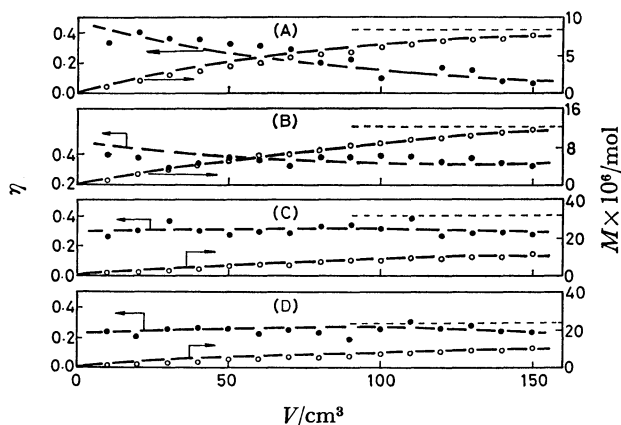


Fig. 10. Relation between rejection and permeate volume.

C_1 : $0.00025 \text{ mol dm}^{-3}$, ----: equilibrium amount adsorbed, M_e , (A): L-glutamic acid, (B): L-aspartic acid, (C): DL-2-aminoadipic acid, (D): DL-2-aminopimelic acid, membrane: DDS-600.

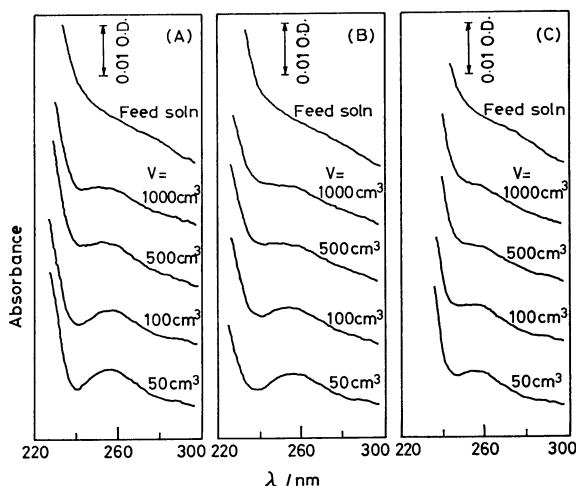


Fig.11. UV spectra of permeate of amino acids. (A): L-Glutamic acid ($C_1=0.001 \text{ mol dm}^{-3}$, $\text{pH}_1=3.72$), (B): L-aspartic acid ($C_1=0.001 \text{ mol dm}^{-3}$, $\text{pH}_1=3.53$), (C): L-glutamic acid ($C_1=0.01 \text{ mol dm}^{-3}$, $\text{pH}_1=3.37$), membrane : laboratory-made.

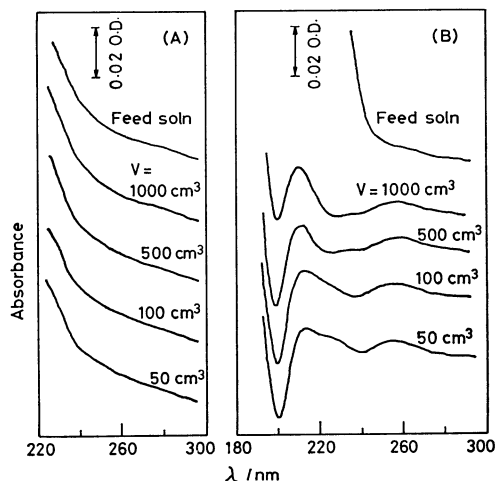


Fig.12. UV spectra of permeate of amino acids. (A): L-Glutamic acid ($C_1=0.001 \text{ mol dm}^{-3}$, $\text{pH}_1=7.0$ by NaOH), (B): L-glutamic acid ($C_1=0.01 \text{ mol dm}^{-3}$, $\text{pH}_1=3.37$), membrane; (A): laboratory-made, (B): DDS-990 ($A=4.2 \times 10^{-5} \text{ mol cm}^{-2} \text{ s}^{-1} \text{ MPa}^{-1}$, $\eta_{\text{NaCl}}=0.89$).

membrane. This happens because the absorption strength of the amino auxochrome is weakened with the decrease of the hydrogen ion concentration in solution by adsorption of hydrogen ions. When the pH of a monoamino dicarboxylic acid aq solution is adjusted to 7 with sodium hydroxide, the hydrogen ions in the solution disappear; as a result, the adsorption does not occur. Therefore, the absorption maxima do not appear in the permeate, as shown in Fig. 12-A. Monoamino dicarboxylic acid permeates, through high-rejection membrane exhibit their absorption maxima in wavelength 212 nm and 255 nm, as shown in Fig. 12-B. Also, the maxima are not inclined to disappear as the permeation proceeds. This is because 1000 cm^3 of the permeate volume is not high enough to attain equilibrium. On the other hand,

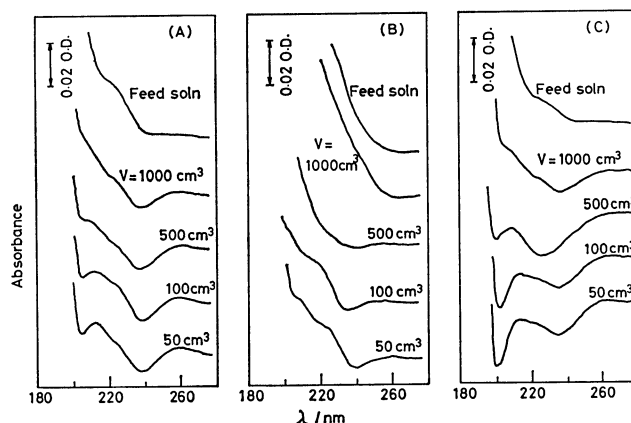


Fig.13. UV spectra of permeate of amino acids. (A): Glycine ($C_1=0.001 \text{ mol dm}^{-3}$, $\text{pH}_1=5.85$), (B): L-alanine ($C_1=0.001 \text{ mol dm}^{-3}$, $\text{pH}_1=5.71$), (C): L-alanine ($C_1=0.001 \text{ mol dm}^{-3}$, $\text{pH}_1=3.80$ by HCl), membrane : laboratory-made.

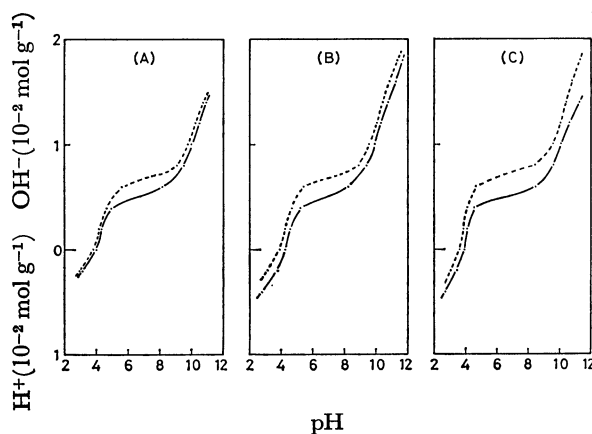


Fig.14. Titration curve of amino acids. (A): L-Glutamic acid ($C=0.00075 \text{ mol dm}^{-3}$), (B): L-glutamic acid ($C=0.00044 \text{ mol dm}^{-3}$), (C): L-aspartic acid ($C=0.00061 \text{ mol dm}^{-3}$), —: permeate, ----: standard soln, membrane; (A): DDS-600, (B),(C): laboratory-made.

the UV spectra of the permeate of some monoamino monocarboxylic acids are shown in Fig. 13. Glycine exhibits an absorption maximum at 211 nm and 260 nm, and L-alanine at 260 nm, but acquires the UV spectrum of the feed solution as the permeation proceeds. In the case of a monoamino monocarboxylic acid, hydrogen ions in zwitter form are adsorbed; as a result, the above maximum appears. When the L-alanine aq solution is acidified with hydrochloric acid, the permeate exhibits its strong absorption maximum at 211 nm and 260 nm. Figure 14 shows the titration curve of monoamino dicarboxylic acids. Here, the amino acid concentration of the permeate is the same as that of a standard solution. The titration curve of the permeate is located below that of the standard solution because the hydrogen ion concentration of the permeate is lower than that of the standard solution. From Fig. 14, it can be seen that the dissociation constants of the amino acids in the permeate is the same as that in the standard solution.

References

- 1) G. Greco, Jr., *Biotechnol. Bioeng.*, **22**, 215 (1980).
 - 2) G. Greco, Jr., D. Albanesi, M. Cantarella, L. Gianfreda, R. Palescandolo, and V. Scardi, *Appl. Microbiol.*, **8**, 249 (1979).
 - 3) D. E. Kohlwey and M. Cheryan, *Enzyme Microb. Technol.*, **3**, 64 (1981).
 - 4) Y. Kiso, T. Kitao, M. Sugihara, and Y. Terashima, *Nippon Kagaku Kaishi*, **1981**, 1805.
 - 5) C. Kamizawa, H. Masuda, and S. Ishizaka, *Bull. Chem. Soc. Jpn.*, **45**, 2964 (1972).
 - 6) P. R. M. Nair, K. C. Patel, and R. D. Patel, *Angew. Makromol. Chem.*, **78**, 109 (1979).
 - 7) M. Tamura, T. Uragami, and M. Sugihara, *Kobunshi*, **36**, 241 (1979).
 - 8) T. Matsuura and S. Sourirajan, *J. Appl. Polym. Sci.*, **16**, 2531 (1972).
 - 9) T. Matsuura and S. Sourirajan, *J. Appl. Polym. Sci.*, **17**, 3683 (1973).
 - 10) S. Sourirajan, *Ind. Eng. Chem., Fundam.*, **2**, 51 (1963).
 - 11) D. Nomura and O. Tozawa, *Maku* (Membrane, in Japanese), **2**, 469 (1977).
 - 12) O. Tozawa and D. Nomura, *Nippon Kagaku Kaishi*, **1978**, 1291.
 - 13) O. Tozawa and D. Nomura, *Nippon Kagaku Kaishi*, **1980**, 127.
 - 14) O. Tozawa and D. Nomura, *Nippon Kagaku Kaishi*, **1981**, 270.
 - 15) S. Kimura and S. Sourirajan, *AIChE J.*, **13**, 497 (1967).
 - 16) S. Manjikian, *Ind. Eng. Chem., Prod. Res. Dev.*, **6**, 23 (1967).
 - 17) T. Matsuura, J. M. Dickson, and S. Sourirajan, *Ind. Eng. Chem., Process Des. Dev.*, **15**, 149 (1976).
 - 18) R. W. Taft, Jr., "Steric Effects in Organic Chemistry," ed by M. S. Newman, Wiley, N. Y. (1956), pp. 598, 608, 619.
 - 19) H. Azumi, "Ryōshi Kagaku," Baifukan, Tokyo (1969), p. 116.
 - 20) T. Matsuura and S. Sourirajan, *J. Appl. Polym. Sci.*, **18**, 3593 (1974).
 - 21) J. R. Pappenheimer, M. P. Lepie, and J. Wyman, Jr., *J. Am. Chem. Soc.*, **58**, 1851 (1936).
 - 22) J. W. Belton, *Trans. Faraday Soc.*, **35**, 1293 (1939).
 - 23) M. E. Heyde, C. R. Peters, and J. E. Anderson, *J. Colloid Interface Sci.*, **50**, 467 (1975).
 - 24) T. Matsuura and S. Sourirajan, *J. Appl. Polym. Sci.*, **17**, 3661 (1973).
 - 25) M. Igawa, S. Yoshida, and T. Yamabe, *Nippon Kagaku Kaishi*, **1975**, 1713.
-